

## Supporting Information

### **Ion-Selective Permeability of Ultrathin Nanoporous Silicon Membrane as Probed by Scanning Electrochemical Microscopy Using Micropipet-Supported ITIES Tips**

Ryoichi Ishimatsu,<sup>†</sup> Jiyeon Kim,<sup>†</sup> Ping Jing,<sup>†</sup> Christopher C. Striemer,<sup>‡</sup> David Z. Fang,<sup>‡</sup>

Philippe M. Fauchet,<sup>‡</sup> James L. McGrath,<sup>§</sup> and Shigeru Amemiya<sup>\*,†</sup>

<sup>†</sup>*Department of Chemistry, University of Pittsburgh, Pittsburgh, Pennsylvania 15260, and* <sup>‡</sup>*Department of Electrical and Computer Engineering, and* <sup>§</sup>*Department of Biomedical Engineering, University of Rochester, Rochester, New York 14627*

<sup>#</sup> Current address: Shandong Entry-Exit Inspection and Quarantine Bureau, P. R. China

\* To whom correspondence should be addressed. E-mail: amemiya@pitt.edu. Fax: 412-624-5259.

**Preparation of Heat-Pulled Micropipets.** The following program was used for a CO<sub>2</sub>-laser capillary puller (model P-2000 Sutter Instrument Co., Novato, CA) to prepare heat-pulled micropipets. A glass capillary was separated during the last line of the program.

Line	Heat	Fil	Vel	Del	Pul
1	470	4	19	150	0
2	460	4	19	150	0
3	450	4	19	150	0
4	440	4	19	150	0
5	430	4	19	150	0
6	420	4	19	150	0

**SICM of FIB-Milled and Non-Milled Micropipets.** SICM approach curves as obtained with FIB-milled and non-milled tips were compared to demonstrate the improved smoothness and alignment of a FIB-milled micropipet (Figure S1). For a comparison, a pair of micropipets was pulled from the same capillary, and the tip of a pipet was milled by FIB. In SICM experiments, the ionic current between a Ag/AgCl electrode inside a water-filled micropipet and a Ag/AgCl electrode placed in the bulk aqueous solution was measured with a bias of 0.3 V between the electrodes. The resulting steady-state current was only 5% larger for the FIB-milled pipet than for the non-milled pipet, thereby confirming a small increase in the tip diameter by FIB milling. As the FIB-milled and non-milled tips approached to a Si wafer substrate, the ionic tip current was eventually blocked by the substrate. The tip current was normalized with respect to the current in the bulk solution so that the approach curves with FIB-milled and non-milled tips partially overlap with each other (Figure S1). This comparison shows

that the FIB-milled tip can approach closer to the substrate to give a lower tip current. Noticeably, the current at the FIB-milled tip decreased only to ~70 % of the current in the bulk solution. The recent theory of SICM suggests that this modest current change is expected at a short tip–substrate distance of <10% of the tip radius.<sup>S1</sup> This result confirms that the glass orifice of a FIB-milled tip can be brought very close to the substrate surface prior to contact. Quantitative understanding of a SICM response, however, requires a more advanced model.<sup>S1</sup>

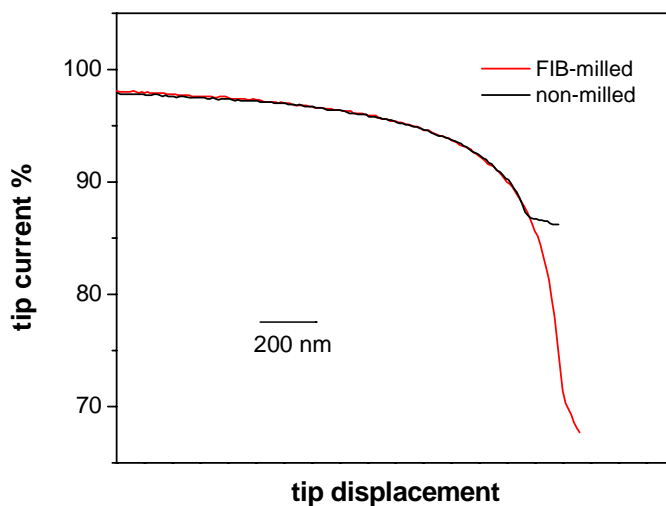


**Figure S1.** SICM approach curves at a SiO<sub>2</sub> substrate as obtained using FIB-milled and non-milled micropipets. Probe scan rate, 0.15 μm/s.

**Finite Element Simulations.** SECM approach curves were simulated by solving the corresponding 2D diffusion problems using the finite element method with COMSOL Multiphysics® version 3.5a (COMSOL, Inc., Burlington, MA) as described elsewhere.<sup>S2</sup> In this work, pipet-supported liquid/liquid interfaces with disk and sphere-cap geometries were considered for monovalent ions and polyions, respectively. The model and boundary conditions are given in Figure 3a. An impermeable membrane was considered to simulate approach curves to SiO<sub>2</sub> substrates. The  $x$  values in eq 1 were calculated by setting  $d/a = 50$ . The example of the simulation for an interface with sphere-cap geometry ( $h/a = 0.38$  for protamine) is attached. In this example, membrane permeability is given by a dimensionless parameter,  $K$ , as

$$K = \frac{ka}{D} \tag{S1}$$

**An Approach Curve as Obtained Using Non-Milled Pipets.** An approach curve to a  $\text{SiO}_2$  substrate as obtained using a non-milled pipet is shown in Figure S2. The surface of non-milled tips is not smooth or perpendicular to the pipet length so that liquid/liquid interfaces supported by the tips do not approach very close to a substrate. Also, the closest distance between the substrate and non-milled tip significantly varies due to the irreproducible roughness and alignment of heat-pulled tips.

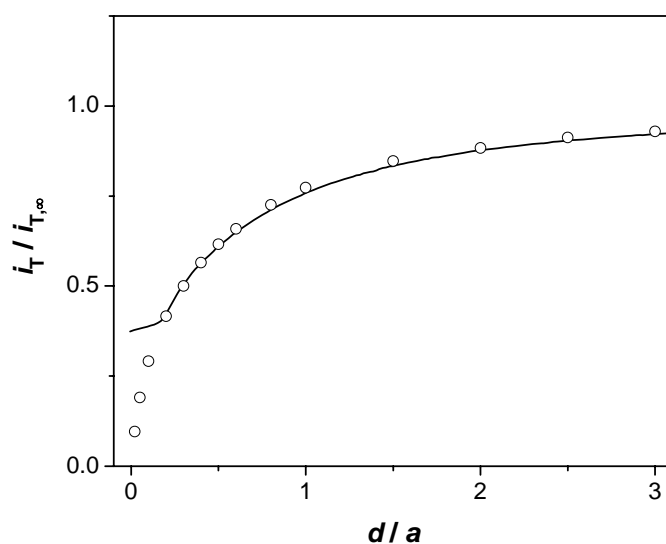


**Figure S2.** SECM approach curve to a  $\text{SiO}_2$  substrate as obtained using a non-milled micropipet for  $\text{TEA}^+$  (solid line). Probe scan rate,  $0.45 \mu\text{m/s}$ . The circles represent an approach curve simulated for an impermeable membrane with  $(a, h/a, r_g/a) = (1.5 \mu\text{m}, 0, 1.2)$ .

**Approach Curves with Protamine in 0.01 M PBS.** Figure S3 shows approach curves to a SiO<sub>2</sub> surface and a pnc-Si membrane in 0.01 M PBS as measured using a FIB-milled pipet when protamine is transferred across the interface (cell 3). The protrusion height of the interfaces is smaller in 0.01 M PBS than in 0.1 or 0.03 M PBS (see Figures 3b and 7).

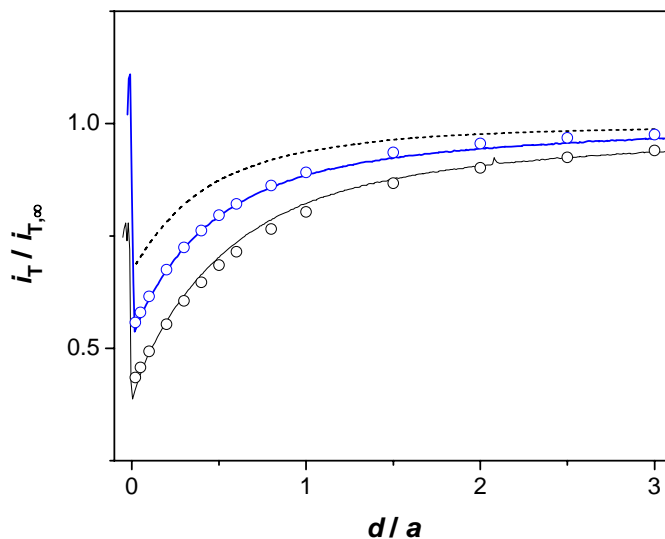


**Figure S3.** Approach curves to a nanopore membrane and a SiO<sub>2</sub> substrate (blue and black lines, respectively) for protamine in 0.01 M PBS. Probe scan rate, 0.23  $\mu\text{m/s}$ . The corresponding circles are simulated approach curves for permeable ( $k = 8.4 \times 10^{-4}$  cm/s) and impermeable membranes for  $(a, h/a, r_g/a) = (2.4 \mu\text{m}, 0.23, 1.2)$  and  $(2.5 \mu\text{m}, 0.23, 1.2)$ , respectively. The dashed line represents an approach curve simulated for diffusion-controlled permeability with  $l = 16$  nm in eq 2 ( $k_d = 2.8 \times 10^{-3}$  cm/s).

**Uniform and Heterogeneous Membrane Models for Derivation of Eq 2.** Eq 2 was derived as follows by considering steady-state ion flux,  $J$ , across the membrane based on uniform and heterogeneous membrane boundary conditions as reported elsewhere<sup>S2</sup> (the left- and right-hand sides of Figure S4, respectively).

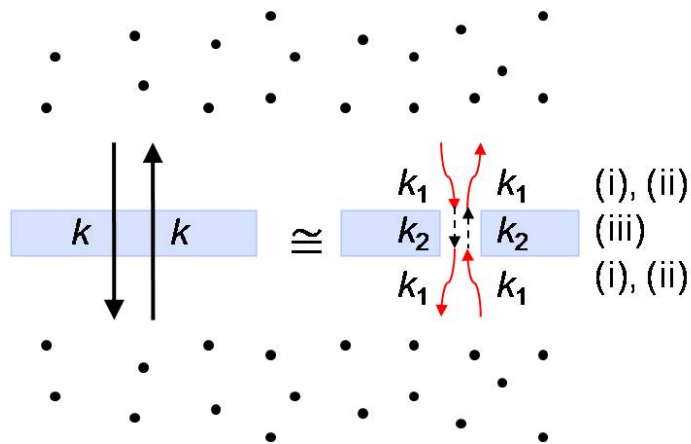


**Figure S4.** Uniform (left) and heterogeneous (right) membrane models used for the definition of membrane permeability.

In the uniform membrane model, the flux is given by membrane permeability,  $k$ , as

$$J = k[c_t(r, 0) - c_b(r, 0)] \quad (\text{S2})$$

where  $c_t(r, 0)$  and  $c_b(r, 0)$  are the concentrations of transported molecules near the membrane at its top- and bottom-solution sides, respectively. Eq S2 is the membrane boundary condition used for the finite element simulation (see above).

In the heterogeneous membrane model, membrane transport is considered as the combination of three diffusion processes, i.e., (i) diffusion from the solution to the pore orifice, (ii) diffusion from the pore orifice to the solution, and (iii) diffusion through the water-filled pores (Figure S4). The second step is a reverse process of the first step and the same rate constant,  $k_1$ , can be assigned to both steps. Moreover, the first step is equivalent to irreversible adsorption of molecules to randomly distributed disks with different radii that cover an impenetrable surface randomly without overlapping.<sup>S2</sup> According to effective medium theories based on Brownian dynamics simulations of this diffusion problem, the corresponding effective reaction rate,  $k_1$ , at the surface with a low surface coverage of the disks is given by<sup>S3</sup>

$$k_1 = 4DN\bar{r} \quad (\text{S3})$$

On the other hand, a rate constant for the third step,  $k_2$ , is given by

$$k_2 = \frac{\sigma D}{l} \quad (\text{S4})$$

Noticeably, ion size and ion–nanopore interaction were assumed to be negligible in this model.

Membrane flux based on the heterogeneous model is given as follows. At the top-solution side of the membrane, ion flux is given by

$$J = k_1[c_t(r, 0) - c_t] \quad (\text{S5})$$

where  $c_t$  is the concentration of transported molecules at the orifice of the nanopores at the top-solution side. This concentration was approximated to be uniform at all nanopores despite their different radii.

Analogously, the flux at the bottom-solution side of the nanopores is given by

$$J = k_1[c_b - c_b(r, 0)] \quad (\text{S6})$$

where  $c_b$  is the concentration of transported molecules at the entrance of the nanopores at the bottom-solution side and is also approximated to be uniform for all pores. Finally, the flux through nanopores is given by

$$J = k_2(c_t - c_b) \quad (\text{S7})$$

Overall, the combination of eqs S5, S6, and S7 gives

$$J = \frac{k_1 k_2}{k_1 + 2k_2} [c_t(r, 0) - c_b(r, 0)] \quad (\text{S8})$$

The comparison of eq S8 with eq S2 gives

$$k = \frac{k_1 k_2}{k_1 + 2k_2} \quad (\text{S9})$$

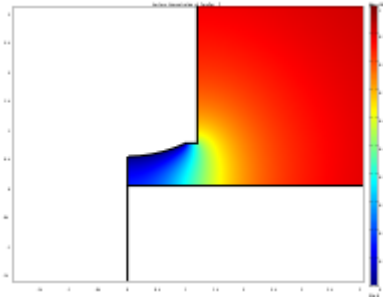
In eq S9,  $k$  becomes equivalent to  $k_d$  when  $k_1$  and  $k_2$  are given by eqs S3 and S4 to represent diffusion-limited permeation, thereby yielding eq 2.

## REFERENCES

- (S1) Edwards, M. A.; Williams, C. G.; Whitworth, A. L.; Unwin, P. R. *Anal. Chem.* **2009**, *81*, 4482–4492.
- (S2) Kim, E.; Xiong, H.; Striemer, C. C.; Fang, D. Z.; Fauchet, P. M.; McGrath, J. L.; Amemiya, S. *J. Am. Chem. Soc.* **2008**, *130*, 4230–4231.
- (S3) Makhnovskii, Y. A.; Berezhkovskii, A. M.; Zitserman, V. Y. *J. Chem. Phys.* **2005**, *122*, 236102 and references cited therein.



# COMSOL Model Report



## 1. Table of Contents

- Title - COMSOL Model Report
- Table of Contents
- Model Properties
- Geometry
- Geom1
- Solver Settings
- Postprocessing
- Equations
- Variables

## 2. Model Properties

Property	Value
Model name	

Author	
Company	
Department	
Reference	
URL	
Saved date	Dec 12, 2009 1:50:21 PM
Creation date	Aug 3, 2007 5:06:17 PM
COMSOL version	COMSOL 3.5.0.608

File name: C:\nanopore.mph

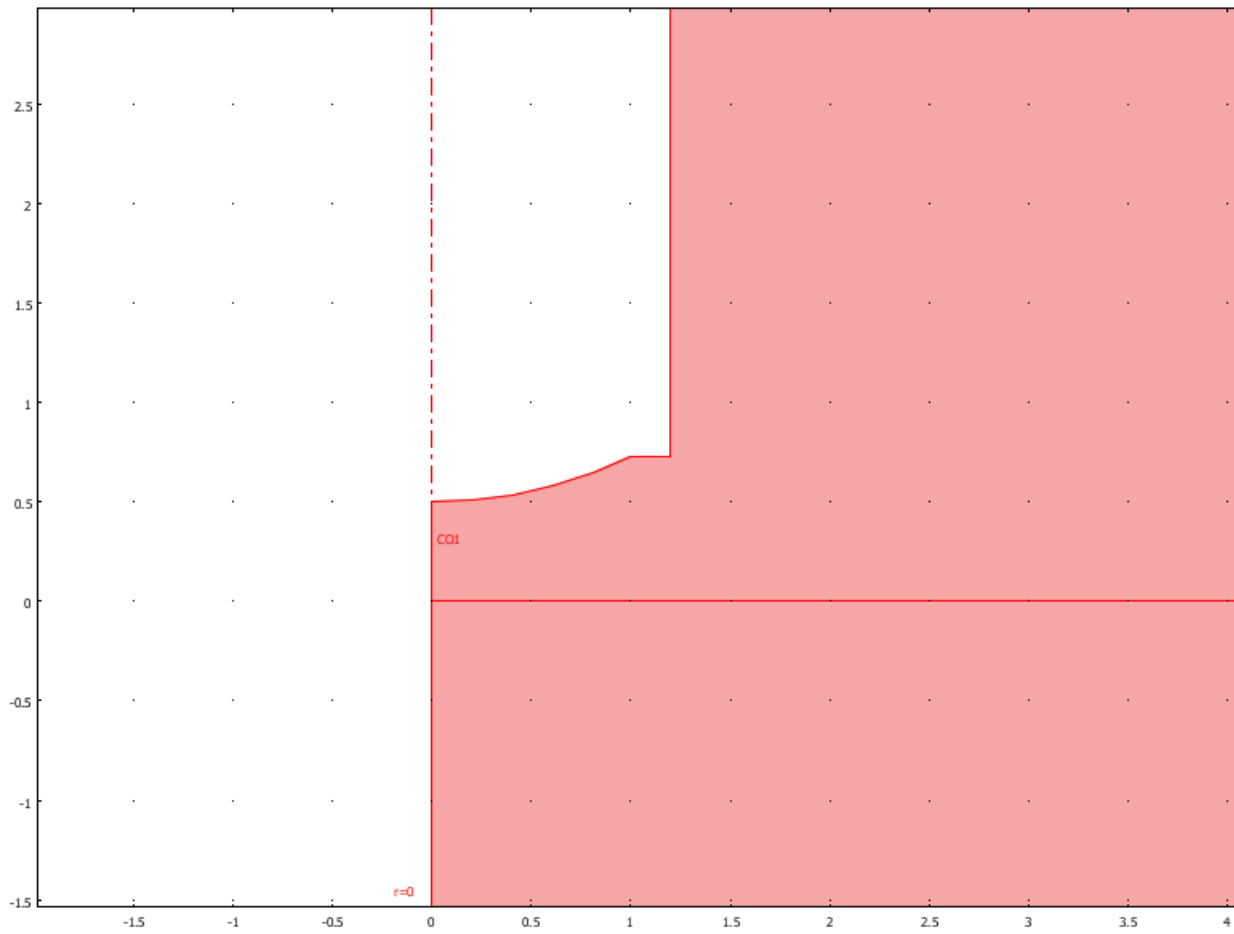
Application modes and modules used in this model:

- Geom1 (Axial symmetry (2D))
  - Diffusion (Chemical Engineering Module)
  - Diffusion (Chemical Engineering Module)

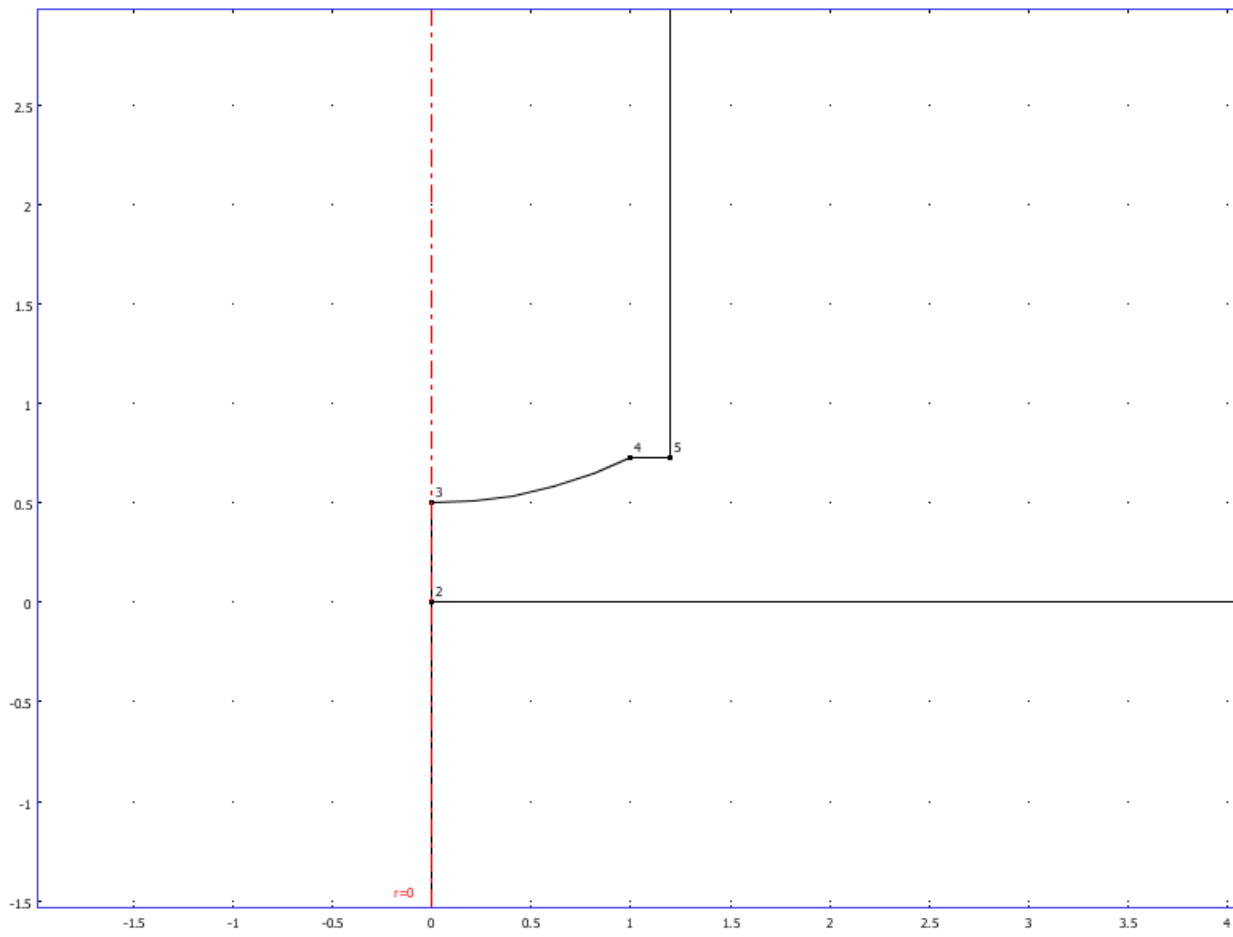
### **3. Geometry**

Number of geometries: 1

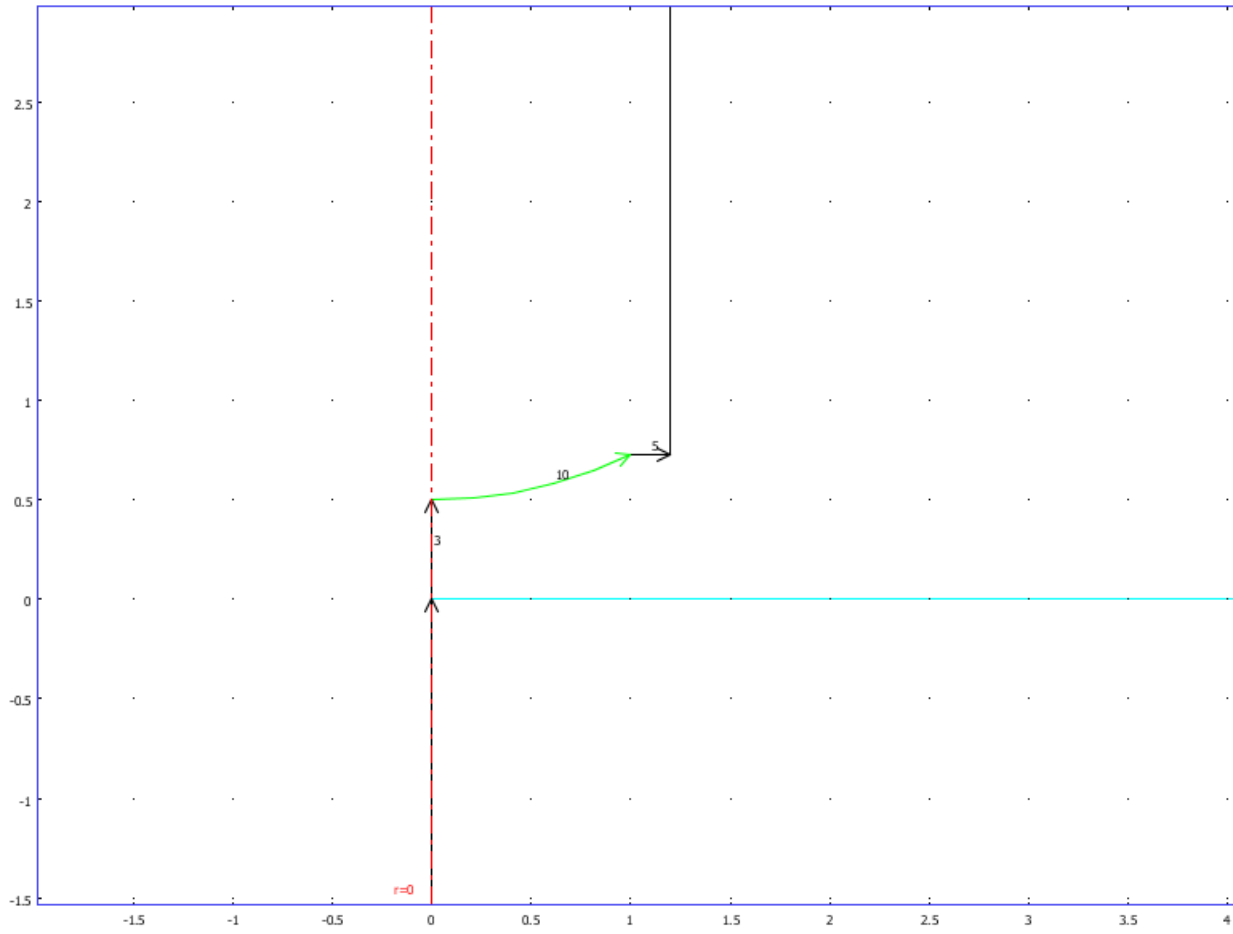
### 3.1. Geom1



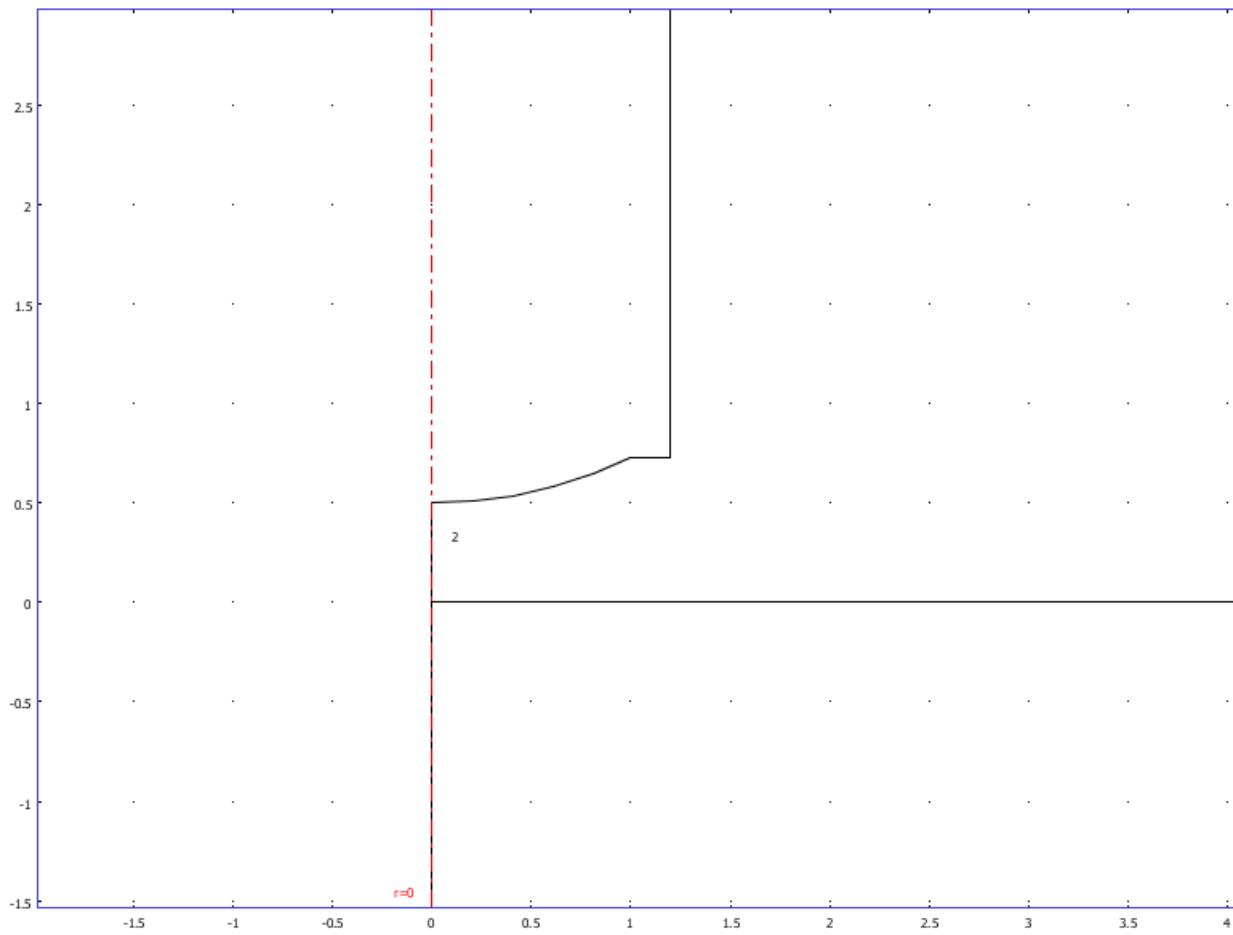
### 3.1.1. Point mode



### 3.1.2. Boundary mode



### 3.1.3. Subdomain mode



## 4. Geom1

Space dimensions: Axial symmetry (2D)

Independent variables: r, phi, z

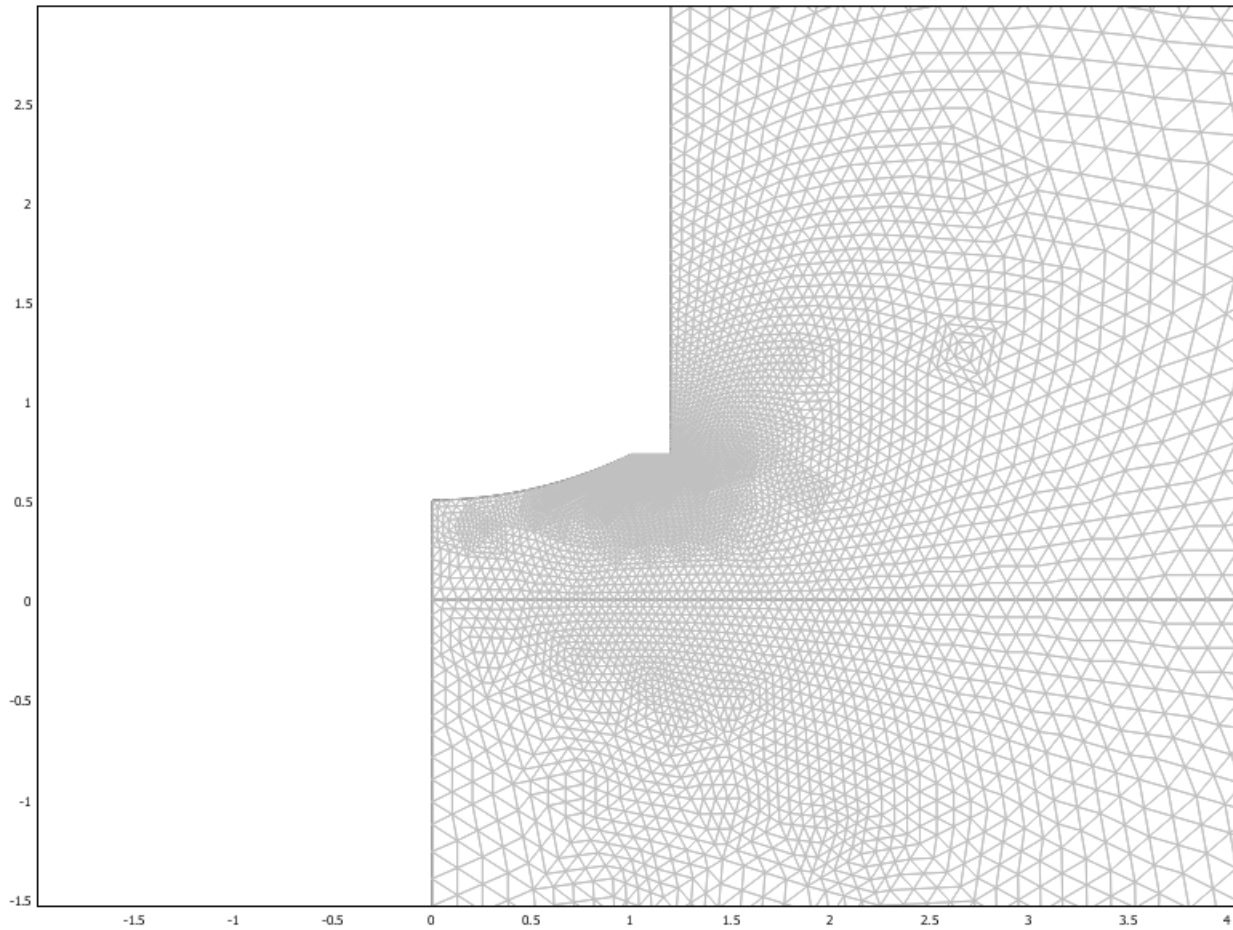
### 4.1. Scalar Expressions

Name	Expression	Unit	Description
K	0.15		

## 4.2. Mesh

### 4.2.1. Mesh Statistics

Number of degrees of freedom	201794
Number of mesh points	50549
Number of elements	100192
Triangular	100192
Quadrilateral	0
Number of boundary elements	1156
Number of vertex elements	9
Minimum element quality	0.829
Element area ratio	0



### ***4.3. Application Mode: Diffusion (chdi)***

Application mode type: Diffusion (Chemical Engineering Module)

Application mode name: chdi

#### **4.3.1. Application Mode Properties**

<b>Property</b>	<b>Value</b>
Default element type	Lagrange - Quadratic
Analysis type	Stationary
Equilibrium assumption	Off
Frame	Frame (ref)

Weak constraints	Off
Constraint type	Ideal

#### 4.3.2. Variables

Dependent variables: c

Shape functions: shlag(2,'c')

Interior boundaries not active

Locked Boundaries: 10

#### 4.3.3. Boundary Settings

Boundary		1	2, 8	4
Type		Axial symmetry	Concentration	Flux
Mass transfer coefficient (kc)	m/s	0	0	<b>0.25*K</b>
Bulk concentration (cb)	mol/m <sup>3</sup>	0	0	<b>c2</b>
Concentration (c0)	mol/m <sup>3</sup>	0	<b>1</b>	0

#### 4.3.4. Subdomain Settings

Subdomain		1
Diffusion coefficient (D)	m <sup>2</sup> /s	<b>0.25</b>
Subdomain initial value		1
Concentration, c (c)	mol/m <sup>3</sup>	1

#### 4.4. Application Mode: Diffusion (chdi2)

Application mode type: Diffusion (Chemical Engineering Module)

Application mode name: chdi2

#### 4.4.1. Application Mode Properties

Property	Value
Default element type	Lagrange - Quadratic
Analysis type	Stationary
Equilibrium assumption	Off
Frame	Frame (ref)
Weak constraints	Off
Constraint type	Ideal

#### 4.4.2. Variables

Dependent variables: c2

Shape functions: shlag(2,'c2')

Interior boundaries not active

Locked Boundaries: 10

#### 4.4.3. Boundary Settings

Boundary		3	4	5-6, 10
Type		Axial symmetry	Flux	Insulation/Symmetry
Mass transfer coefficient (kc)	m/s	0	<b>0.25*K</b>	0
Bulk concentration (cb)	mol/m <sup>3</sup>	0	<b>c</b>	0
Concentration (c0)	mol/m <sup>3</sup>	0	0	0
Boundary		7, 9		
Type		Concentration		
Mass transfer coefficient (kc)	m/s	0		

Bulk concentration (cb)	mol/m <sup>3</sup>	0
Concentration (c0)	mol/m <sup>3</sup>	1

#### 4.4.4. Subdomain Settings

Subdomain		2
Diffusion coefficient (D)	m <sup>2</sup> /s	<b>0.25</b>
Subdomain initial value		2
Concentration, c2 (c2)	mol/m <sup>3</sup>	1

## 5. Solver Settings

Solve using a script: off

Analysis type	Stationary
Auto select solver	On
Solver	Stationary
Solution form	Automatic
Symmetric	auto
Adaptive mesh refinement	Off
Optimization/Sensitivity	Off
Plot while solving	Off

### 5.1. Direct (UMFPACK)

Solver type: Linear system solver

Parameter	Value
Pivot threshold	0.1

Memory allocation factor	0.7
--------------------------	-----

### ***5.2. Stationary***

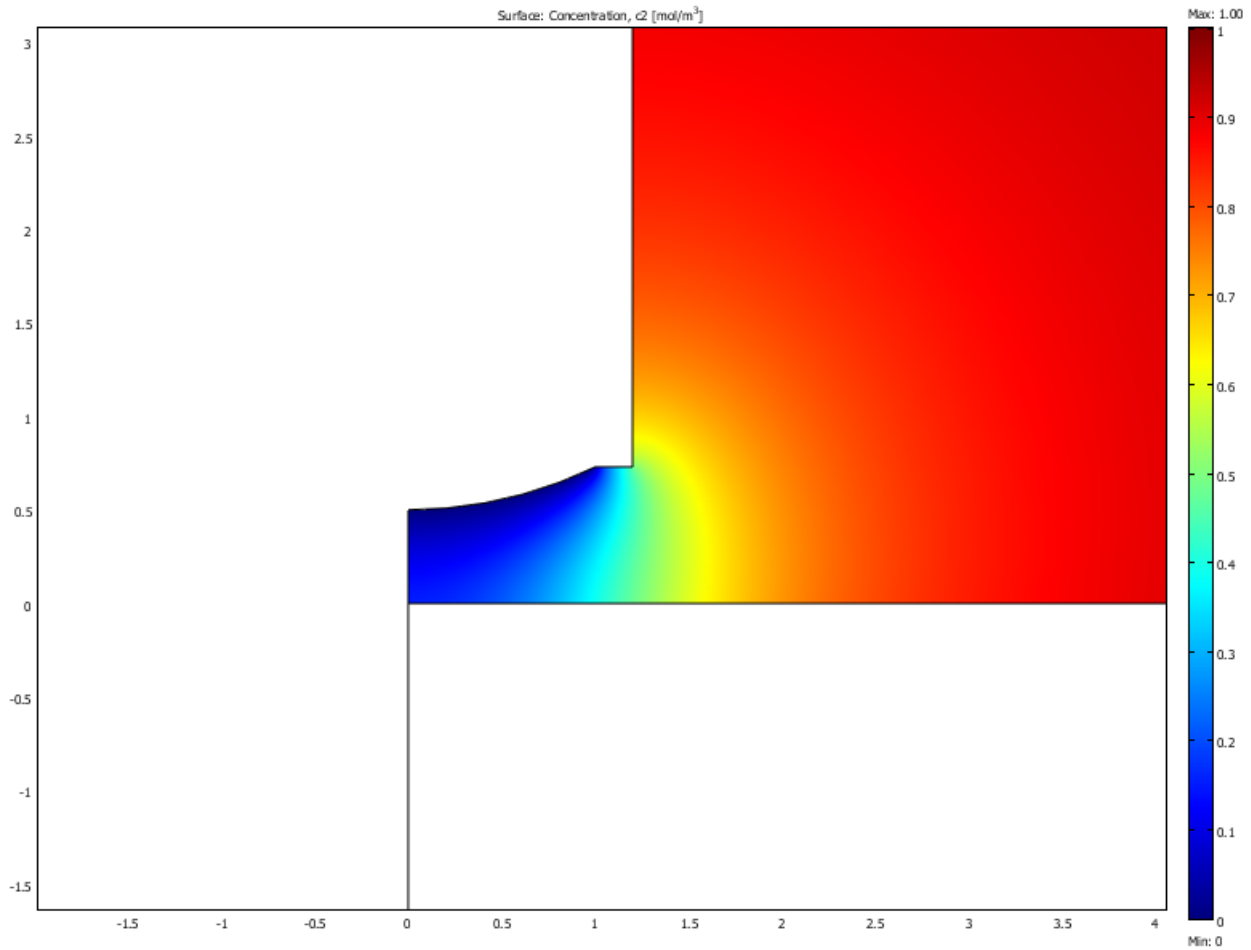
<b>Parameter</b>	<b>Value</b>
Linearity	Automatic
Relative tolerance	1.0E-6
Maximum number of iterations	25
Manual tuning of damping parameters	Off
Highly nonlinear problem	Off
Initial damping factor	1.0
Minimum damping factor	1.0E-4
Restriction for step size update	10.0

### ***5.3. Advanced***

<b>Parameter</b>	<b>Value</b>
Constraint handling method	Elimination
Null-space function	Automatic
Automatic assembly block size	On
Assembly block size	5000
Use Hermitian transpose of constraint matrix and in symmetry detection	Off
Use complex functions with real input	Off
Stop if error due to undefined operation	On
Store solution on file	Off

Type of scaling	Automatic
Manual scaling	
Row equilibration	On
Manual control of reassembly	Off
Load constant	On
Constraint constant	On
Mass constant	On
Damping (mass) constant	On
Jacobian constant	On
Constraint Jacobian constant	On

## 6. Postprocessing



## 7. Equations

### 7.1. Boundary

Dependent variables: c, c2

#### 7.1.1. Boundary: 10

h coefficient

c	c2
0	0

-d(-c2,c)	-d(-c2,c2)
-----------	------------

r coefficient

0
-c2

## 8. Variables

### 8.1. Boundary

#### 8.1.1. Boundary 1-2, 8

Name	Description	Unit	Expression
ndflux_c_chdi	Normal diffusive flux, c	mol/(m <sup>2</sup> *s)	nr_chdi * dflux_c_r_chdi+nz_chdi * dflux_c_z_chdi
ndflux_c2_chdi2	Normal diffusive flux, c2	mol/(m <sup>2</sup> *s)	

#### 8.1.2. Boundary 3, 5-7, 9-10

Name	Description	Unit	Expression
ndflux_c_chdi	Normal diffusive flux, c	mol/(m <sup>2</sup> *s)	
ndflux_c2_chdi2	Normal diffusive flux, c2	mol/(m <sup>2</sup> *s)	nr_chdi2 * dflux_c2_r_chdi2+nz_chdi2 * dflux_c2_z_chdi2

#### 8.1.3. Boundary 4

Name	Description	Unit	Expression
ndflux_c_chdi	Normal diffusive	mol/(m <sup>2</sup> *s)	nr_chdi * dflux_c_r_chdi+nz_chdi *

	flux, c		dflux_c_z_chdi
ndflux_c2_chdi2	Normal diffusive flux, c2	mol/(m <sup>2</sup> *s)	nr_chdi2 * dflux_c2_r_chdi2+nz_chdi2 * dflux_c2_z_chdi2

## 8.2. Subdomain

### 8.2.1. Subdomain 1

Name	Description	Unit	Expression
grad_c_r_chdi	Concentration gradient, c, r component	mol/m <sup>4</sup>	cr
dflux_c_r_chdi	Diffusive flux, c, r component	mol/(m <sup>2</sup> *s)	-Drr_c_chdi * cr-Drz_c_chdi * cz
grad_c_z_chdi	Concentration gradient, c, z component	mol/m <sup>4</sup>	cz
dflux_c_z_chdi	Diffusive flux, c, z component	mol/(m <sup>2</sup> *s)	-Dzr_c_chdi * cr-Dzz_c_chdi * cz
grad_c_chdi	Concentration gradient, c	mol/m <sup>4</sup>	sqrt(grad_c_r_chdi <sup>2</sup> +grad_c_z_chdi <sup>2</sup> )
dflux_c_chdi	Diffusive flux, c	mol/(m <sup>2</sup> *s)	sqrt(dflux_c_r_chdi <sup>2</sup> +dflux_c_z_chdi <sup>2</sup> )
grad_c2_r_chdi2	Concentration gradient, c2, r component	mol/m <sup>4</sup>	

dflux_c2_r_chdi2	Diffusive flux, c2, r component	mol/(m <sup>2</sup> *s)	
grad_c2_z_chdi2	Concentration gradient, c2, z component	mol/m <sup>4</sup>	
dflux_c2_z_chdi2	Diffusive flux, c2, z component	mol/(m <sup>2</sup> *s)	
grad_c2_chdi2	Concentration gradient, c2	mol/m <sup>4</sup>	
dflux_c2_chdi2	Diffusive flux, c2	mol/(m <sup>2</sup> *s)	

### 8.2.2. Subdomain 2

Name	Description	Unit	Expression
grad_c_r_chdi	Concentration gradient, c, r component	mol/m <sup>4</sup>	
dflux_c_r_chdi	Diffusive flux, c, r component	mol/(m <sup>2</sup> *s)	
grad_c_z_chdi	Concentration gradient, c, z component	mol/m <sup>4</sup>	
dflux_c_z_chdi	Diffusive flux, c, z component	mol/(m <sup>2</sup> *s)	

grad_c_chdi	Concentration gradient, c	mol/m <sup>4</sup>	
dflux_c_chdi	Diffusive flux, c	mol/(m <sup>2</sup> *s)	
grad_c2_r_chdi2	Concentration gradient, c2, r component	mol/m <sup>4</sup>	c2r
dflux_c2_r_chdi2	Diffusive flux, c2, r component	mol/(m <sup>2</sup> *s)	-Drr_c2_chdi2 * c2r-Drz_c2_chdi2 * c2z
grad_c2_z_chdi2	Concentration gradient, c2, z component	mol/m <sup>4</sup>	c2z
dflux_c2_z_chdi2	Diffusive flux, c2, z component	mol/(m <sup>2</sup> *s)	-Dzr_c2_chdi2 * c2r-Dzz_c2_chdi2 * c2z
grad_c2_chdi2	Concentration gradient, c2	mol/m <sup>4</sup>	sqrt(grad_c2_r_chdi2 <sup>2</sup> +grad_c2_z_chdi2 <sup>2</sup> )
dflux_c2_chdi2	Diffusive flux, c2	mol/(m <sup>2</sup> *s)	sqrt(dflux_c2_r_chdi2 <sup>2</sup> +dflux_c2_z_chdi2 <sup>2</sup> )